



Tomato methionine sulfoxide reductase B2 functions in drought tolerance by promoting ROS scavenging and chlorophyll accumulation through interaction with Catalase 2 and RBCS3B

Long Cui^{a,1}, Fangyan Zheng^{a,1}, Dedi Zhang^a, Changxing Li^a, Miao Li^a, Jie Ye^a, Yuyang Zhang^a, Taotao Wang^a, Bo Ouyang^a, Zonglie Hong^b, Zhibiao Ye^a, Junhong Zhang^{a,*}

^a The Key Laboratory of Horticultural Plant Biology, Ministry of Education, Huazhong Agricultural University, Wuhan 430070, China

^b Department of Plant Sciences, University of Idaho, Moscow, ID 83844, USA

ARTICLE INFO

Keywords:

Catalase
Chlorophyll
Methionine sulfoxide reductase
Rubisco small subunit
Tomato

ABSTRACT

Reactive oxygen species (ROS) are inevitably generated in aerobic organisms as by-products of common metabolism and as the result of defense and development. ROS readily oxidizes methionine (Met) residues of proteins to form Met-R-sulfoxide or Met-S-sulfoxide (MetSO), resulting in protein inactivation or malfunction. Although it is known that MetSO can be reverted to Met by methionine sulfoxide reductase (Msr), the mechanism how Msr interacts with its target proteins is poorly understood. In this study, two target proteins of tomato MsrB2 (SIMsrB2), catalase 2 (CAT2) and the Rubisco small subunit RBCS3B, were identified. Silencing of *SIMsrB2* by RNA interference (RNAi) in tomato led to decreased drought tolerance, accompanied by increased ROS accumulation and chlorophyll degradation. By contrast, overexpression of *SIMsrB2* in tomato significantly reduced ROS accumulation and enhanced drought tolerance. Protein interaction analysis showed that SIMsrB2 interacts with CAT2 and RBCS3B *in vitro* and *in planta*. Silencing of *CAT2* by RNAi and *RBCS3B* by virus-induced gene silencing (VIGS) resulted in development of pale green leaves and enhanced ROS accumulation in tomato plants. These results demonstrate that SIMsrB2 functions in drought tolerance and promotes chlorophyll accumulation by modulating ROS accumulation.

1. Introduction

Tomato is one of the most important vegetable crops cultivated worldwide. Adversities, which often trigger production of ROS (reactive oxygen species), could severely reduce the tomato fruit yield and quality by limiting plant growth and development. Therefore, improvement of the crop's tolerance to stress has become an urgent challenge facing the tomato industry [1].

ROS are widely produced as common byproducts of various metabolic pathways in plants and animals. Methionine (Met) and cysteine (Cys) residues of proteins are common targets of ROS. The oxidation of Cys residues is known to be highly related to the ROS level and its oxidation can transduce the redox signal to the downstream cellular events including the redox-based post-translational modifications of key residues of proteins [2]. ROS can attack proteins by inducing oxidation of methionine residues (Met) to Met sulfoxide (MetSO) [3]. Met is one of

the most sensitive amino acids in proteins to oxidation, and its oxidation to MetSO leads to changes in peptide hydrophobicity, alterations in protein conformation, and even loss of biological activity of proteins [4–6]. To counteract the toxicity arising from Met oxidation, living organisms have evolved methionine sulfoxide reductase (Msr) to repair the oxidized Met, by reducing MetSO back to Met [4,6,7]. Msr also participates in the scavenging of ROS and reactive nitrogen intermediates in cells by reversible oxidation/reduction of Met in proteins [8].

There are two isozymes of Msr, MsrA and MsrB, which are stereospecific for conversion of the *S* and *R* diastereomers of MetSO, respectively [7]. The first identified substrate of MsrA in plants was Hsp21, a chloroplast-localized small heat shock protein [9]. Hsp21 can be sulfoxidized in the conserved N-terminal region that is highly rich in Met residues. The oxidized Hsp21 can be reduced by the plastidic MsrA, which restores in its function as a molecular chaperone that helps protein folding under stress conditions [9]. *Arabidopsis* mutant of the

* Corresponding author.

E-mail address: zhangjunhng@mail.hzau.edu.cn (J. Zhang).

¹ These authors contributed equally to this work.

cytosolic MsrA gene (*Msr2*) shows reduced growth and slower development under short-day, but not long-day conditions [10].

The first plant MsrB homolog was identified by in silico search of the human selenoproteinX-like proteins in the *Arabidopsis* genome [11]. There are two chloroplastic *MsrB* genes in *Arabidopsis* and only one in rice (*Oryza sativa*). These genes exhibit differential expression patterns in different plant tissues and respond differently to various stressor treatments [12]. The most ubiquitously expressed *MsrB* shows enhanced expression in response to plant dehydration and oxidative stress, and the *MsrB* mutants of *Arabidopsis* accumulate higher levels of oxidized Met upon exposure to oxidative stress. In pepper, the *CaMsrB2* gene has been shown to be a novel defense regulator against oxidative stress and pathogen attack [13]. These studies suggest that MsrB is involved in the response to oxidative stress [12,14,15]. However, the molecular mechanisms underlying oxidative stress responses and the possible interacting proteins of MsrB2 in repairing the oxidized Met have not been resolved.

H₂O₂ is an important signaling molecule regulating the processes of plant development, stress adaptation and programmed cell death (PCD) [16]. There are multiple pathways of H₂O₂ production in plant cells, including enzymatic and non-enzymatic reactions, such as photorespiration, electron transport chains, and redox reactions. Chloroplasts and mitochondria are two main organelles for production of endogenous H₂O₂ in plant cells [17,18]. To overcome the oxidative stress by H₂O₂, almost all organisms have evolved the ability to break down H₂O₂ into H₂O and O₂ in the presence of catalase [16]. In eukaryotic organisms, catalase is mainly located in the peroxisomes, thus widely considered as a peroxisome marker enzyme [19]. Unlike in animals, there are multiple genes encoding catalase in plants, for example, *CAT1*, *CAT2* and *CAT3* in *Arabidopsis*. Genetic studies have shown that catalase enzyme activity is reduced significantly in *cat2* mutant, but only slightly in *cat3*, whereas deletion of *CAT1* has no observable effect on the catalase enzyme activity [16,20,21]. Proteins that have recently been reported to interact with catalase, thus affecting its enzyme activity, include no catalase activity 1 (NCA1), calmodulin, triple gene block protein 1 (TGB1), nucleoside diphosphate kinase 1 (NDK1) and lesion simulating disease 1 (LSD1) [21–26].

Ribulose 1,5-bisphosphate carboxylase/oxygenase (Rubisco) is the most abundant protein on earth and also a very (if not the most) important enzyme to the life of green plants. In fact, almost all organic carbons found in the living beings ultimately come from atmospheric CO₂ that is fixed by this enzyme. Rubisco is a potential target for genetic manipulation to increase crop yield [27,28]. Rubisco is also one of the largest enzyme complexes in plants, with molecular mass of 560 kD [29]. It is composed of eight small subunits coded by the nuclear *RBCS* multigene family and eight large subunits coded by the *RbcL* gene in the plastid genome [30]. There are four *RBCS* members in *Arabidopsis*, *RBCS1A*, *RBCS1B*, *RBCS2B* and *RBCS3B* [29], among which *RBCS3B* is synthesized in the cytoplasm and transported to the chloroplast, where it is assembled into the Rubisco complex with other subunits [29]. *RBCS3B* plays a very important role for the maintenance of leaf photosynthetic capacity. Co-suppression of *RBCS3B* in *Arabidopsis* shows typical albino or pale green (*apg*) phenotypes and ROS accumulation in leaves [29].

In this study, we report that *SlMsrB2* positively regulates ROS scavenging and chlorophyll contents in tomato leaves. Suppression of *MsrB2* expression was found to lead to chlorophyll degradation and ROS accumulation in tomato leaves under drought conditions. Less ROS accumulation and significantly improved drought tolerance were observed in *MsrB2* overexpression transgenic lines. Yeast two-hybrid experiments and co-immunoprecipitation (CoIP) assays showed that *MsrB2* directly interacts with *CAT2* and *RBCS3B*. Knock-down of *CAT2* expression by RNAi leads to development of transgenic tomato plants with pale green leaves and ROS accumulation, and suppression of *RBCS3B* by virus-induced gene silencing (VIGS) also leads to formation of tomato pale green leaves. Taken together, our results demonstrate that *MsrB2*, an ROS damage repair enzyme in tomato, interacts with

CAT2 and *RBCS3B* and restore their oxidized methionine (Met) residues, to regenerate their activity under drought stress. Our findings provide new insights on how *MsrB2* improves tomato drought tolerance by regulating ROS accumulation.

2. Materials and methods

2.1. Plant materials and growth conditions

Wild type (WT) tomato cultivar Ailsa Craig (AC) was used for transformation experiments. Plants of the WT (AC) and transgenic lines were grown in nutrition pots in a greenhouse at the campus of Huazhong Agricultural University in Wuhan (30.4°N, 114.2°E), China. *Nicotiana benthamiana* and tomato VIGS plants were grown in an environmentally controlled room at 22 °C with a photoperiod of 16 h light/8 h darkness.

2.2. RNA isolation and gene expression analysis

Total RNA was extracted from various tissues of the transgenic lines or WT plants using the TRIZOL reagent (Invitrogen, USA). Complementary DNAs were synthesized using an M-MLV reverse transcriptase kit (Toyobo, Japan). The LightCycler480 SYBR Green I Master Kit (Roche Applied Sciences, Germany) was used for the qPCR analysis. Three biological replicates from each genotype were analyzed to test for statistical differences. The tomato *Actin* gene (BT013524) was used as the internal control. The primer sequences used in real-time PCR are listed in Table S1.

2.3. Vector construction and tomato transformation

The full-length open reading frame (ORF) and RNAi sequences of *SlMsrB2* and *SlCatalase2* were amplified from tomato cDNA using the KOD-Plus DNA polymerase (Toyobo, Japan), and cloned into specific target vectors, respectively. The constructed vectors were introduced into *Agrobacterium tumefaciens* strain C58 and used for tomato transformations according to the method described previously [31]. Genomic DNA was extracted from transgenic plants using the CTAB method as described by Murray and Thompson (1980). The genomic DNA was analyzed by PCR for presence of markers to confirm their transgenic plant identity. Sequences of all the primers used in these experiments are listed in Table S1.

2.4. Yeast two-hybrid assay

The full-length ORF of *MsrB2* was amplified from tomato cDNA and cloned into pGBKT7 (Clontech, USA). The full-length ORFs of *Catalase2* and *RBCS3B* were amplified from tomato cDNA and cloned into pGADT7 (Clontech, USA). The primer sequences are provided in Table S1. Both vectors of *MsrB2*-pGBKT7 and *Catalase2*-pGADT7 and the combination of *MsrB2*-pGBKT7 + *RBCS3B*-pGADT7 were introduced into the Y2H gold yeast strain (Clontech, USA), respectively, and cultured on synthetic dropout (SD)/-Trp-Leu medium. Negative and positive control vectors were also introduced into Y2H gold yeast and cultured on SD/-Trp-Leu. After 3–5 days of growth, yeast colonies were picked up and suspended in 0.9% NaCl to an OD₆₀₀ of 0.1. The suspension (2 μL) was spotted on SD/-Trp-Leu and SD/-Trp-His-Leu-Ade medium, respectively. The plates were incubated for 3–7 days in an incubator at 30 °C.

2.5. Transient expression in tobacco leaves

The full-length ORF of *MsrB2* without the stop codon was amplified and cloned into the effector vectors Ph7LIC-6Flag, nEYFP and 101YFP, respectively. The full-length ORF of *Catalase2* and *RBCS3B* without the stop codon were amplified and cloned into mCherry76, cEYFP and Ph7LIC-6Myc vectors. In each vector, the cauliflower mosaic virus (CaMV) 35 S promoter was used to drive the gene expression.

A. tumefaciens GV2260 was transformed with the effector and reporter vectors, respectively, and used to transfect tobacco leaves. For subcellular localization assays, two days after *Agrobacterium* inoculation, fluorescence from the transformed tobacco leaves was imaged using a confocal laser scanning microscope (Leica, TCS SP2). For co-immunoprecipitation assays, transformed tobacco leaf tissue was collected and stored in liquid nitrogen. The leaf samples were added to 1 mL of protein extraction buffer (50 mM Tris-HCl, pH 7.5, 150 mM NaCl, 5 mM EDTA, 2 mM DTT, 10% glycerol, 1% polyvinylpyrrolidone, plant protease inhibitor cocktail (Sigma-Aldrich)) to extract total proteins. The supernatant was incubated with 15 μ L of anti-FLAG affinity matrix (MBL, Japan) at 4 °C for 2 h to capture the tagged protein. The resulting matrix was washed five times with washing buffer (50 mM Tris-HCl, pH 7.5, 250 mM NaCl, 5 mM EDTA, 10% glycerol, 1 mM PMSF), and the protein complex was analyzed by SDS-PAGE and immunoblotting. All primers used for the construction of the vectors are listed in Table S1.

2.6. VIGS analysis in tomato plants

The coding regions (CDS) of the *RBCS3B* and *phytoene desaturase* (*PDS*) genes were amplified by PCR and fused to the effector vector TRV2. *A. tumefaciens* GV2260 was separately transformed with the effector and reporter vectors. Seven-day-old tomato Ailsa Craig (AC) seedlings were selected for *RBCS3B* silencing assays. Single colonies of *Agrobacterium* transformed with genes were grown overnight in 5 mL of LB (5 g yeast extract/L, 10 g peptone/L, 10 g NaCl/L) medium containing rifampicin (50 mg/mL) and kanamycin (100 mg/mL). The transformed *Agrobacterium* cells were harvested and washed by IM (20 mM MES, 10 mM MgCl₂, 0.1 mM acetosyringone). *Agrobacterium* containing TRV1 and *Agrobacterium* containing either TRV2, TRV2-PDS, or TRV2-RBCS3B were mixed at a 1:1 ratio and then infiltrated into the cotyledons of 7-d-old tomato seedlings. 20 seedlings were used for *RBCS3B* and *PDS* gene silencing experiments, respectively. After 20 d of inoculation, leaf tissues were collected for gene expression detection and plants were used for phenotyping observations. All experiments were repeated at least three times. The sequences of primers used in this experiment are listed in Table S1.

2.7. Chlorophyll content measurement

A sample of 0.1 g leaf tissue was harvested from each transgenic and WT plant. Leaf samples were homogenized in 1 mL of 80% methanol and extracted for 3 h in dark. The leaf extracts were centrifuged at 10,000 rpm for 15 min at 4 °C. The supernatants were collected for chlorophyll content measurements by spectrophotometry at 663 and 645 nm. Total chlorophyll was calculated in fresh weight as described by Lichtenthaler and Wellburn (1985) [32].

2.8. DAB staining

In situ generation of H₂O₂ was detected by histochemical staining with DAB [33]. The stained leaves were transferred to a destaining solution consisting of 95% ethanol in a water bath at 95 °C for 10 min and kept in 70% ethanol until imaging.

2.9. Water loss measurement

To detect the rate of water loss under dehydration conditions, the third fully-expanded leaves from the top of the plants were detached from the transgenic and wild-type plants and weighed immediately on a piece of weighing paper. The leaves were then placed on a filter paper and dehydrated at room temperature in dark. The weight was recorded at the indicated intervals. The rate of water loss was calculated as the loss in the initial fresh weight of the samples at each time point [34].

2.10. CAT activity assays

The CAT activity was measured by using the ammonium molybdate method (Nanjing Jiancheng, A007-1-1). Leaf samples were collected and ground to powder with liquid nitrogen. The leaf powder samples were homogenized with saline solution in the ratio of 1 (g): 9 (mL). After centrifugation at 2500 rpm, the supernatant was transferred for determination in a microplate reader. CAT activity (U/mg) was calculated as (Control OD value–Determine OD value) \times 235.65 \times 1/ (60 \times sample mass)/ Protein concentration (mg/mL).

2.11. Measurement of relative electrolyte leakage

Relative electrolyte leakage, which provides a measure of cellular membrane integrity, is frequently used to evaluate plant drought tolerance [35]. The upper second fully-expanded leaves from drought-stressed and non-stressed transgenic and wild-type plants were excised and used to generate leaf discs (8 mm in diameter). Twenty leaf discs per replicate and three replicates for each line were used for assays. The leaf discs were placed into 50 mL centrifuge tubes containing 25 mL distilled deionized water and shaken at 60 rpm for 12 h in dark at 25 °C. Electrolyte leakage (R1) in the solution was measured with a portable magnetic conductivity meter (DDB-303A, Shanghai, China) at 25 °C. These solutions were boiled for 30 min and cooled to room temperature. The electrolyte leakage of the boiled solution (R2) was determined. Relative electrolyte leakage (%) was calculated as (R1/R2) \times 100.

2.12. Statistical analysis

Statistical analyses were conducted using SigmaPlot, Excel and the SPSS (IBM, SPSS 22) software. Comparisons between pairs of the groups were performed using the Student's *t*-test. Statistically significant differences were categorized into two groups: $P < 0.05$ and $P < 0.01$.

2.13. Accession Numbers

The gene sequences used in our experiments are available from the Sol Genomics Network databases using the following accession numbers: *SIMsrB2*, Solyc10g047930; *SlCatalase2*, Solyc12g094620 and *SlRBCS3B*, Solyc02g085950.

3. Results

3.1. *MsrB2* is a chloroplast localized protein

Pepper *CaMsrB2* protein contains 185 amino acid residues and has been shown to regulate ROS accumulation [13,36]. *SIMsrB2*, the ortholog of *CaMsrB2* in tomato, encodes a protein of 197 amino acid residues. A search of protein databases revealed that *SIMsrB2* contains the typical four conserved motifs in a SelR domain (Fig. 1a). The SelR domain of *SIMsrB2* contains a conserved 119-amino acid region (76–194). To examine the phylogenetic relationship of homologous proteins in the *Msr* family, we retrieved 9, 4 and 4 protein sequences, respectively, from the databases of *Arabidopsis* (Araport11), pepper (*Capsicum annuum* release 1.55 DB) and tomato (SIITAG release 4.0 DB). From the phylogenetic tree (Fig. 1b), we found that *SIMsrB2* and *CaMsrB2* were more homologous to each other than to *AtMsrB2*, which formed a separate clade. The *Arabidopsis* *MsrB* members (paralogs) were clustered together, but were, however, distributed away from those of pepper and tomato (Fig. 1B). Multiple sequence alignment showed that *SIMsrB2* shared high sequence similarity at the C terminus with *CaMsrB2* (93%), *AtMsrB2* (82%), and *NtMsrB2* (78%), whereas their N-terminal regions were less conserved (Fig. 1a).

We examined the expression patterns of *SIMsrB2* in various tomato organs. *SIMsrB2* was expressed in all tissues examined, with the highest expression level in leaves, flowers and young fruits (Fig. 2a). To

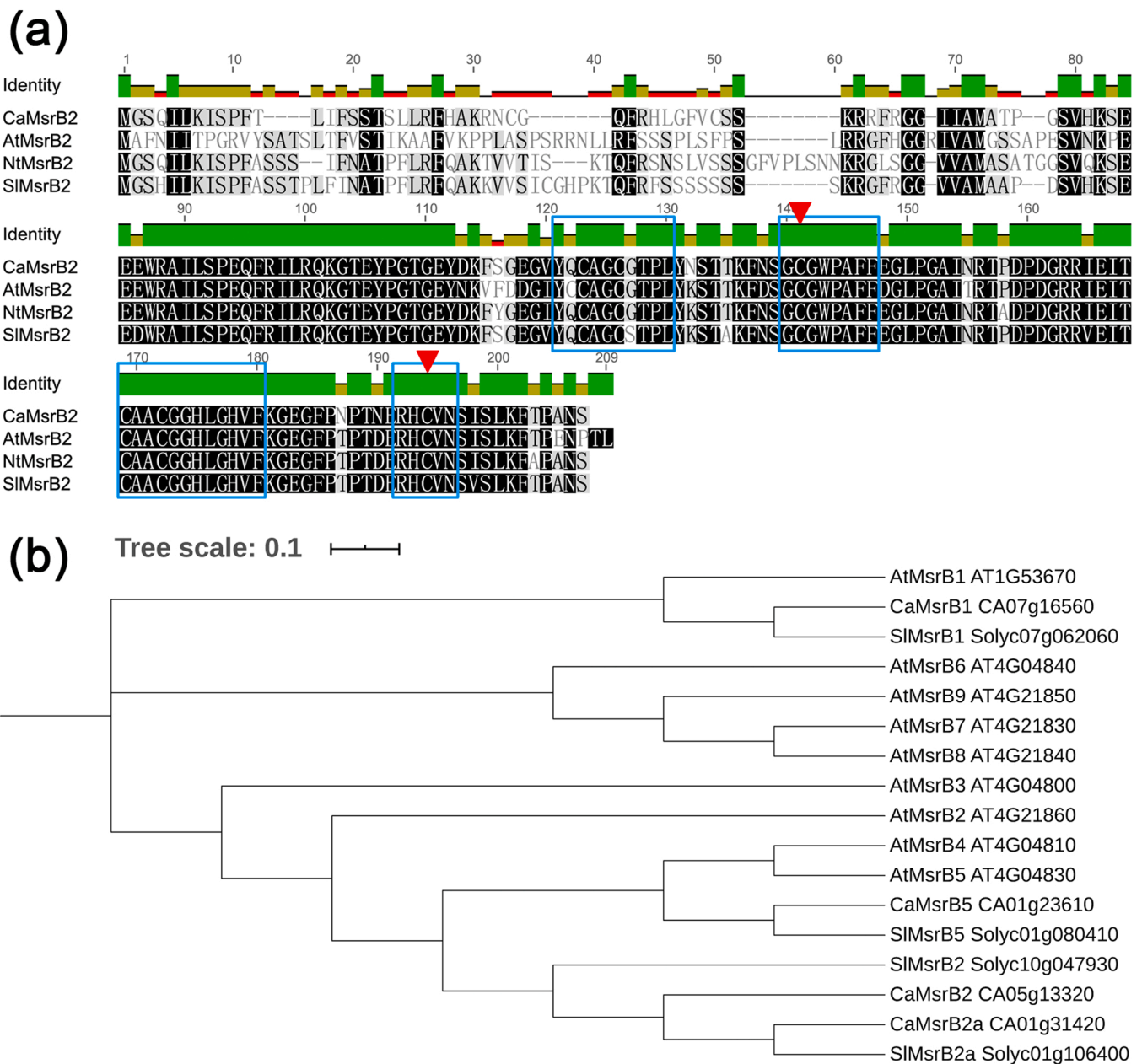


Fig. 1. Characterization of tomato MsrB2. (a) Multiple sequence alignment of MsrB2 orthologs from pepper (Ca), *Arabidopsis* (At), tobacco (Nt) and tomato (Sl). Four putative MSRB signature motifs are boxed, and two highly conserved Cys residues are indicated with red arrowheads. (b) Phylogenetic tree of MsrB homologs from *Arabidopsis thaliana* (At), *Capsicum annuum* (Ca) and *Solanum lycopersicum* (Sl).

determine the subcellular localization of the SIMsrB2 protein, a fusion protein of SIMsrB2 with yellow fluorescence protein (YFP) was expressed under the control of the CaMV 35S promoter in *N. benthamiana* (Fig. 2b). Confocal laser scanning microscopy revealed that the yellow fluorescence of the MsrB2-YFP fusion protein was present in a punctate pattern in the cytoplasm of the cell, which completely overlapped with the red autofluorescence from the chloroplasts (Fig. 2c), suggesting that MsrB2 is localized to the chloroplast. Based on these observations, we concluded that tomato MsrB2 accumulates in the chloroplast.

3.2. SIMsrB2 is involved in drought response

To examine the role of SIMsrB2, its overexpression (OE) and RNA interference (RNAi), transgenic tomato lines were generated. Two OE lines with significantly higher SIMsrB2 expression than the wild-type

(WT) control and three RNAi lines with significantly lower SIMsrB2 expression (Fig. 2d-e) were selected for further analysis. There was no visible phenotypic difference among the OE, RNAi lines and WT plants under normal growth conditions. However, under drought stress, the OE lines were more resistant to drought stress than the WT plants, whereas the RNAi lines were more sensitive to drought stress as compared to the WT plants (Fig. 3a). Further investigations revealed that higher chlorophyll content was detected in the OE lines and lower one appeared in the RNAi lines under drought stress (Fig. 3b). Consistent with the phenotypes under drought stress, the water loss rate in leaves was significantly higher in the RNAi lines while lower in the OE lines as compared to the WT plants (Fig. 3c). The DAB staining assay was used to measure the ROS content. The results illustrated that there was no significant difference in ROS content between the transgenic lines and the WT plants under normal growth conditions, but more ROS was produced in the RNAi lines and less in the OE lines under drought conditions

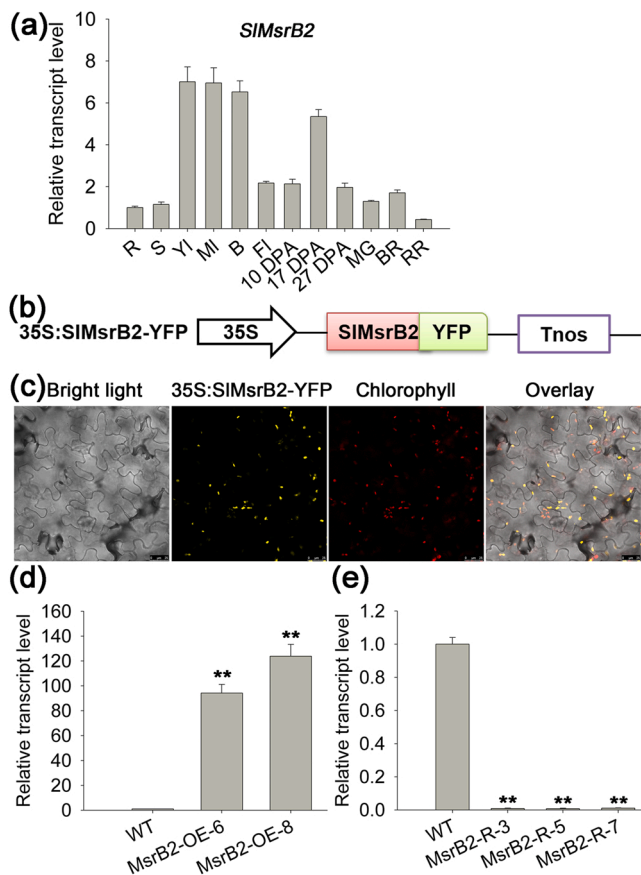


Fig. 2. Subcellular localization and gene expression of SIMsrB2. (a) Transcript levels of *MsrB2* in different tomato organs. R, root; S, stem; Yl, young leaf; ML, mature leaf; B, bud; Fl, flower; 10 DPA, ten days post anthesis; 17 DPA, 17 days post anthesis; 27 DPA, 27 days post anthesis; MG, mature green stage fruit; BR, breaker stage fruit; RR, red ripe stage fruit. All samples were collected at nine weeks after planting. (b) Plasmid construct used for subcellular localization of MsrB2. The expression of MsrB2-YFP was driven by the CaMV 35 S. Tnos, 3'-transcription terminator of the nopaline synthase (*NOS*) gene. (c) Transient expression of 35 S::MsrB2-YFP in tobacco (*N. benthamiana*) leaves. Fluorescence images were acquired using a confocal laser scanning microscope (Leica TCS SP2) 24–48 hrs after infiltration with *Agrobacterium*. Chloroplast auto-fluorescence (red) was used as a control. Bars, 25 μ m. (d–e) Quantitative RT-PCR analysis of *MsrB2* expression in young leaves of WT tomato plants, two *MsrB2*-overexpressing lines (MsrB2-OE-6 and MsrB2-OE-8) and three *MsrB2*-RNAi lines (MsrB2-R-3, MsrB2-R-5 and MsrB2-R-7). Leaf tissues were collected 20 days after planting. Three replicate experiments were performed. The bars represent mean values \pm SE. Asterisks (**) indicate statistical significance at $P < 0.01$.

(Fig. 3d). Consistently, there was no significant difference in relative electrolyte leakage between the transgenic and WT plants under normal conditions (Fig. 3e). There was a remarkable increase in the relative electrolyte leakage in both the transgenic lines and the WT plants 7 days after drought treatment as compared to those under the normal growth conditions. It is interesting and important to note that under drought conditions, the levels of the relative electrolyte leakage was significantly lower in the OX lines, while higher in RNAi lines than in the WT control (Fig. 3e). Similarly, the catalase activity level was significantly higher in the OX lines while lower in the RNAi lines than that in the WT control only under drought stress (Fig. 3f). These results suggested that SIMsrB2 is involved in ROS scavenging in tomato plants under drought stress. Taken together, these results revealed that SIMsrB2 participates in drought responses, and plays an important role in ROS scavenging and chlorophyll accumulation in tomato plants under drought stress conditions.

3.3. SIMsrB2 interacts with CAT2 and RBCS3B

In order to explore the molecular mechanism of SIMsrB2 on ROS scavenging and chlorophyll accumulation under drought stress, a yeast two-hybrid (Y2H) assay was performed to examine whether SIMsrB2 interacted with two potential protein partners, CAT2 and RBCS3B. As expected, both CAT2 and RBCS3B interacted strongly with SIMsrB2 in Y2H assays (Fig. 4a). To further confirm these interactions *in planta*, a co-immunoprecipitation (CoIP) assay was performed. For this experiment, SIMsrB2 was expressed as a fusion protein with the FLAG tag, whereas CAT2 and RBCS3B were tagged with the Myc epitope. We used anti-FLAG antibodies to immunoprecipitate SIMsrB2-FLAG and then used anti-Myc antibodies to detect the interaction proteins (CAT2-Myc or RBCS3B-Myc) on Western blots. The results showed that both CAT2-Myc and RBCS3B-Myc could be pulled down by anti-FLAG antibodies and detected in the immunoprecipitates derived from plant tissues expressing SIMsrB2-FLAG and CAT2-Myc or RBCS3B-Myc (Fig. 4b). This result indicates that both CAT2 and RBCS3B can stably interact with SIMsrB2 in plant cells. The interaction between MsrB2 and CAT2 was further confirmed using the BiFC (bimolecular fluorescence complementation) assay (Fig. 4c). We first expressed tomato CAT2 as a YFP-tagged protein to compare its subcellular localization with the known Arabidopsis peroxisome marker AtCAT2 as an RFP-tagged protein in tobacco leaf cells. Confocal laser scanning microscopy revealed that the yellow fluorescence of the SiCAT2-YFP fusion protein was present in a punctate pattern in the cytoplasm of the cell, which completely overlapped with the red auto-fluorescence from the peroxisome-marker AtCAT2-RFP (Fig. S1), suggesting that tomato SiCAT2 is localized to the peroxisome. We then co-expressed the tomato MsrB2 and CAT2 as fusion proteins with the N-terminal YFP and C-terminal YFP, respectively, for reconstitution of yellow fluorescence when the two proteins interacted with each other. Our BiFC result showed that when MsrB2-nYFP and CAT2-cYFP were co-expressed, yellow fluorescence was reconstituted and observed in a punctate pattern (Fig. 4c, YFP), which was consistent with the red fluorescence signals from AtCAT2-RFP (Fig. 4c, RFP). This BiFC result clearly showed that MsrB2 and CAT2 interacted with each other in the peroxisome (Fig. 4c). To determine whether SIMsrB2 co-localized with RBCS3B protein in the same organelle inside the cell, we co-expressed RBCS3B as a fusion protein with RFP and MsrB2 as a fusion protein with YFP in tobacco leaf cells. Our results of confocal laser scanning microscopy showed that MsrB2-YFP and RBCS3B-RFP were found to co-localize to the chloroplast (indicated by arrows in Fig. 4d). Taken together, our results show that SIMsrB2 can directly interact with CAT2 and RBCS3B *in vitro* and *in planta*.

3.4. ROS and chlorophyll accumulation are modulated in transgenic plants with down-regulated expression of CAT2 or RBCS3B

To test whether CAT2 and RBCS3B play a similar role as MsrB2 in ROS scavenging and chlorophyll accumulation, respectively, we generated transgenic tomato plants with overexpression (OE) and RNA interference (RNAi) of CAT2. Three OE lines with significantly higher CAT2 expression than WT and three RNAi lines with significantly lower CAT2 expression were selected for further analysis (Fig. 5a). Compared with the WT plants, the leaf color of RNAi transgenic lines was pale green (Fig. 5c–d, S2), and the chlorophyll content was significantly reduced (Fig. 5b). Analysis of the DAB staining results revealed that ROS was accumulated in CAT2 RNAi lines (Fig. 5e). The sepals and the shoulders of young fruits were unevenly pale green in CAT2 RNAi lines (Fig. S3a–b), and unevenly green or yellow spots appeared on the shoulders of red ripe fruits (Fig. S3c–d). The CAT2 OE lines, however, did not show visible phenotypic changes (data not shown).

To investigate the importance of RBCS3B in defense against oxidative stress and maintenance of chloroplasts during drought, we performed VIGS (virus induced gene silencing) experiments to silence the expression of RBCS3B. We included PDS-VIGS as control (Fig. 6a–c).

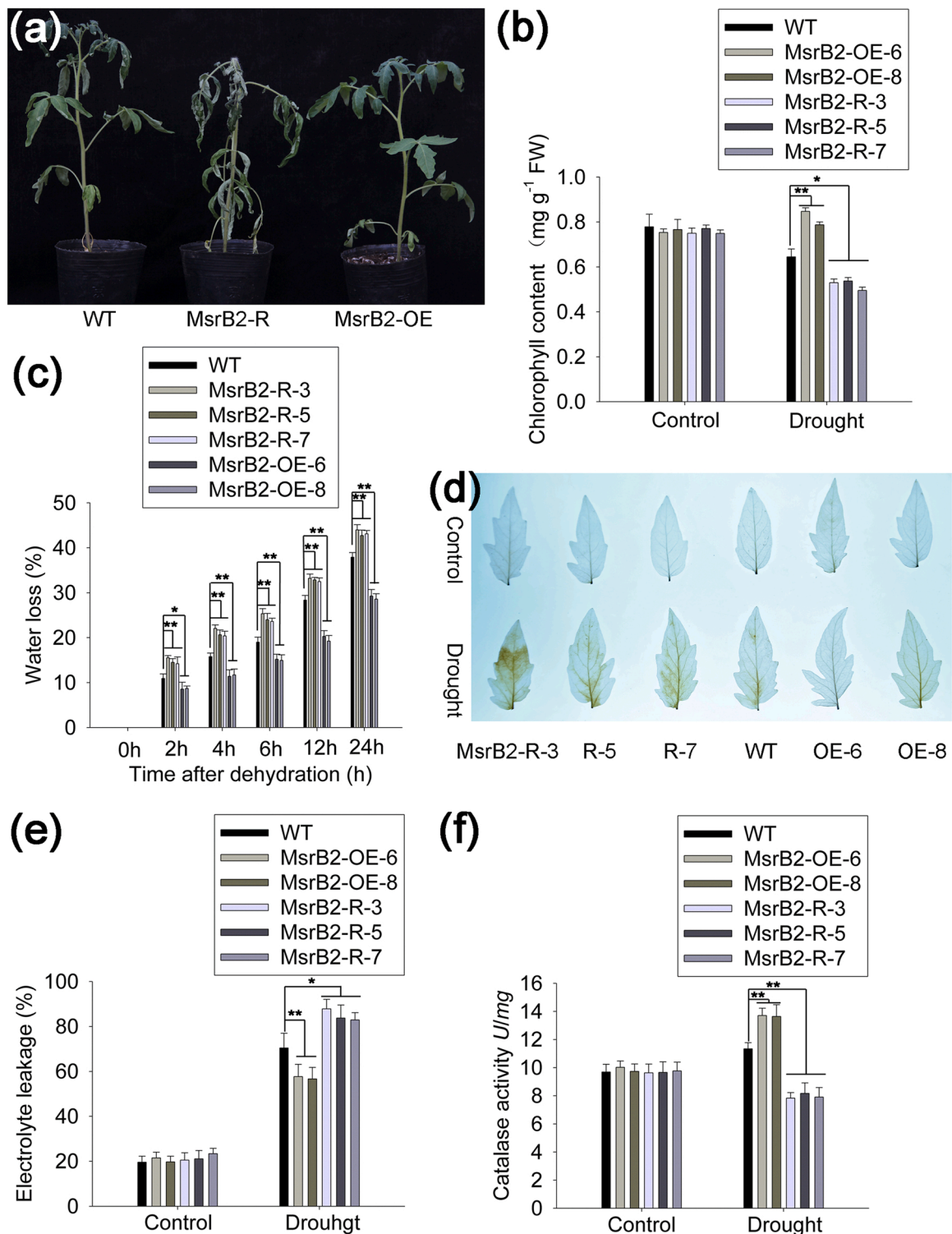
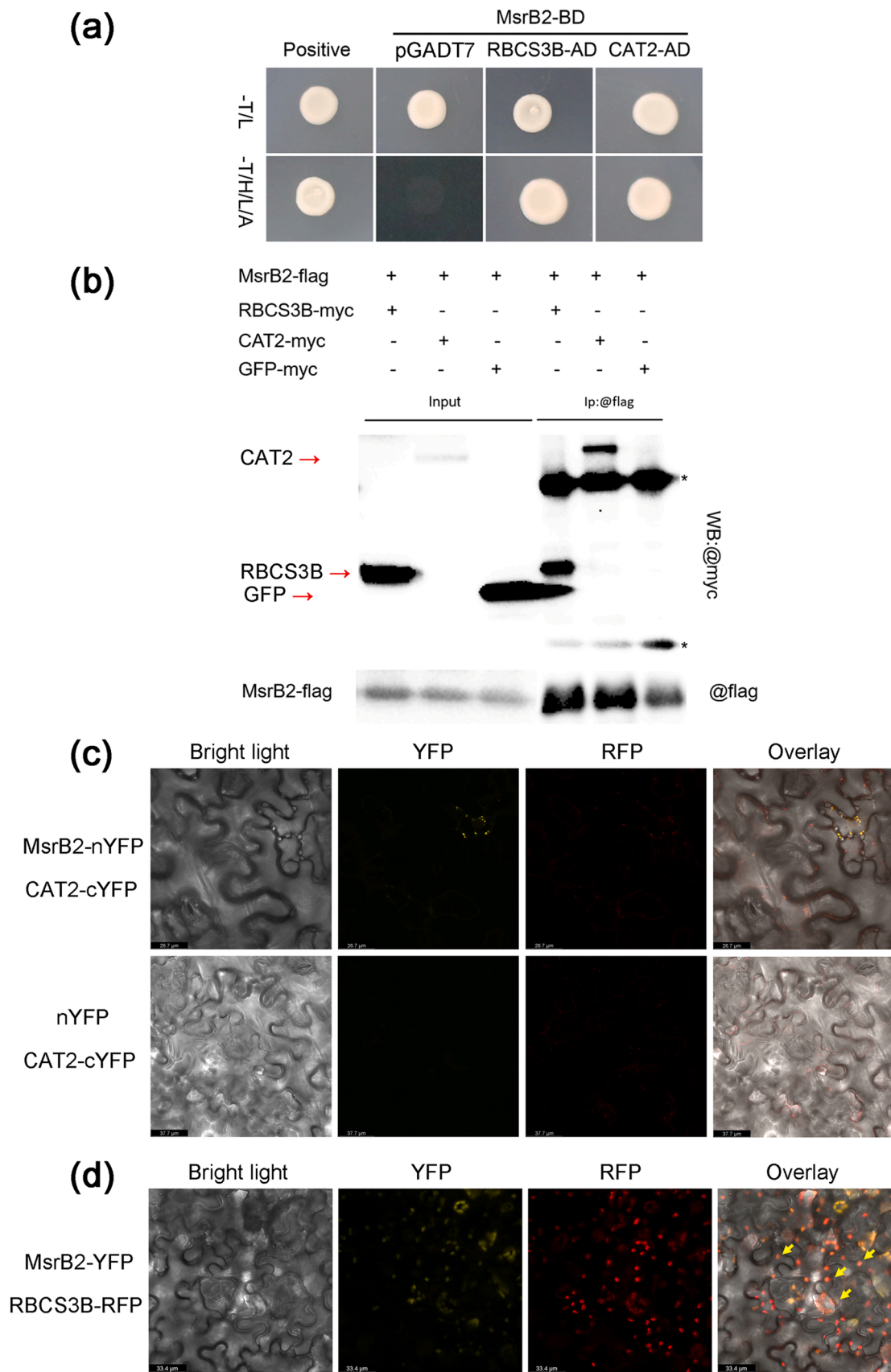


Fig. 3. Drought and dehydration tolerance assays of transgenic tomato plants. (a) Phenotypes of wild-type (WT) tomato and transgenic lines expressing *MsrB2* RNAi (MsrB2-R) or overexpressing *MsrB2* (MsrB2-OE) 7 days after the onset of drought stress. (b) Chlorophyll contents of 30-d-old wild-type (WT) tomato and transgenic lines expressing *MsrB2* RNAi (MsrB2-R-3, -5 and -7) or overexpressing *MsrB2* (MsrB2-OE-6 and -8) grown in normal and drought stress conditions for 7 days. (c) Water loss from the detached leaves of transgenic lines and WT tomato plants. Water loss is presented as the percentage of the initial fresh weight at each time point. (d) Detection of H_2O_2 by DAB staining under normal and drought conditions in transgenic lines and WT. Brown spots indicate polymerization of DAB in the presence of H_2O_2 . (e-f) Relative electrolyte leakage (e) and catalase activity (f) in leaves of transgenic lines and wild-type plants grown in optimal and drought stress conditions. For b, c, e and f, mean values with standard errors (\pm SE) were taken from three replicates, and asterisks (* and **) indicate statistical significance at $P < 0.05$ and 0.01 , respectively.



(caption on next page)

Fig. 4. Interaction of MsrB2 with Catalase 2 and RBCS3B. (a) Interactions in the yeast two-hybrid system. Yeast cells containing pGBKT7-MsrB2 + pGADT7-CAT2, pGBKT7-MsrB2 + pGADT7-RBCS3B, pGBKT7-53 + pGADT7-RecT (positive control) and pGBKT7-MsrB2 + pGADT7 (negative control) were tested for interactions on SD/-Trp/-Leu and SD/-Trp/-Leu/-His/-Ade media. (b) Analysis of protein interactions using co-immunoprecipitation (co-IP). Anti FLAG antibodies were used for co-IP from leaf extracts containing MsrB2-FLAG + CAT2-Myc, MsrB2-FLAG + RBCS3B-Myc and MsrB2-FLAG + GFP-Myc (negative control). Immunoprecipitates were analyzed on Western blots with anti Myc antibodies (top panel) or anti-FLAG antibodies (lower panel). Arrows indicate the positions of CAT2, RBCS3B and GFP. (c) Verification of interaction between SlMsrB2 and SlCatalase2 *in planta* using the BiFC method. MsrB2 was fused to the N-terminal fragment of YFP and CAT2 was fused to the C-terminal YFP. The two fusion proteins were co-expressed in tobacco leaves. Co-expression of CAT2-cYFP and the empty vector (nYFP) served as a negative control. Note that reconstituted yellow fluorescence (YFP) was observed in a punctate pattern that did not overlap with the chloroplast red autofluorescence (RFP) in tobacco leaf cells expressing SlCatalase2-cYFP and nYFP-SlMsrB2, suggesting that the two proteins interact in the peroxisomes. (d) Colocalization of MsrB2 and RBCS3B *in planta*. Confocal micrographs were taken using bright light, or using proper filters for YFP and RFP. Yellow arrows indicate colocalization of YFP and RFP proteins.

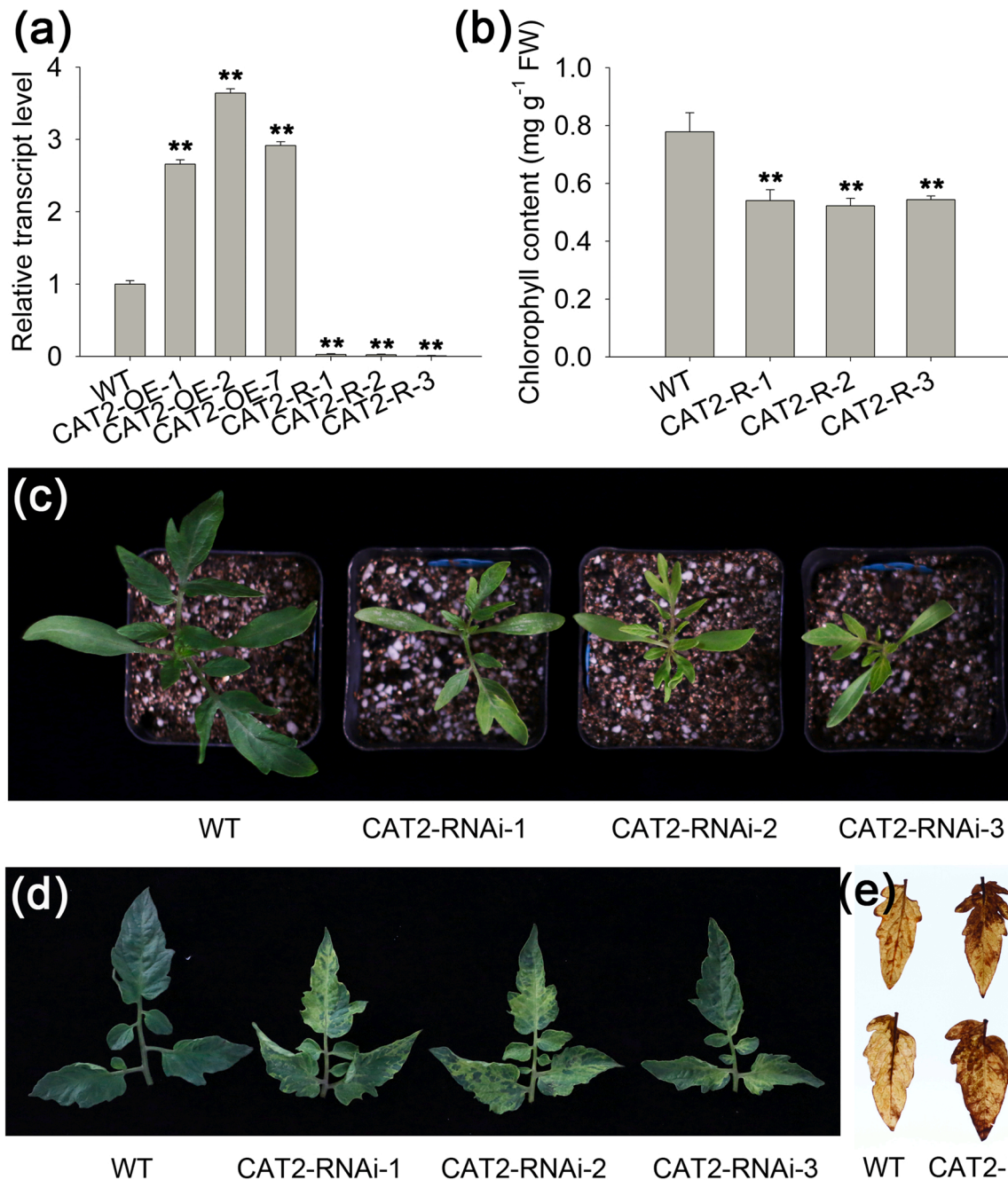


Fig. 5. Transgenic tomato plants expressing *CAT2*-RNAi or overexpressing *CAT2*. (a) Quantitative RT-PCR analysis of *CAT2* expression in young leaves of wild type (WT) tomato plants and transgenic lines overexpressing *SlCAT2* (CAT2-OE-1 and -2) or expressing *SlCAT2*-RNAi (CAT2-RNAi-1, -2 and -3). Leaf tissues were collected 20 days after planting. (b) Chlorophyll contents were measured from leaf samples of 30-day-old wild-type (WT) tomato plants and *CAT2*-RNAi transgenic lines. For a and b, error bars represent mean values \pm SE (n = 3) and ** indicate statistical significance at $P < 0.01$. (c-d) Phenotypes of tomato plants and leaves in *SlCAT2*-RNAi lines and WT control. (e) Detection of H₂O₂ by DAB staining in old leaves of *SlCAT2*-RNAi transgenic lines and WT control. Brown spots indicate polymerization of DAB in the presence of H₂O₂. The leaves were collected nine weeks after planting.

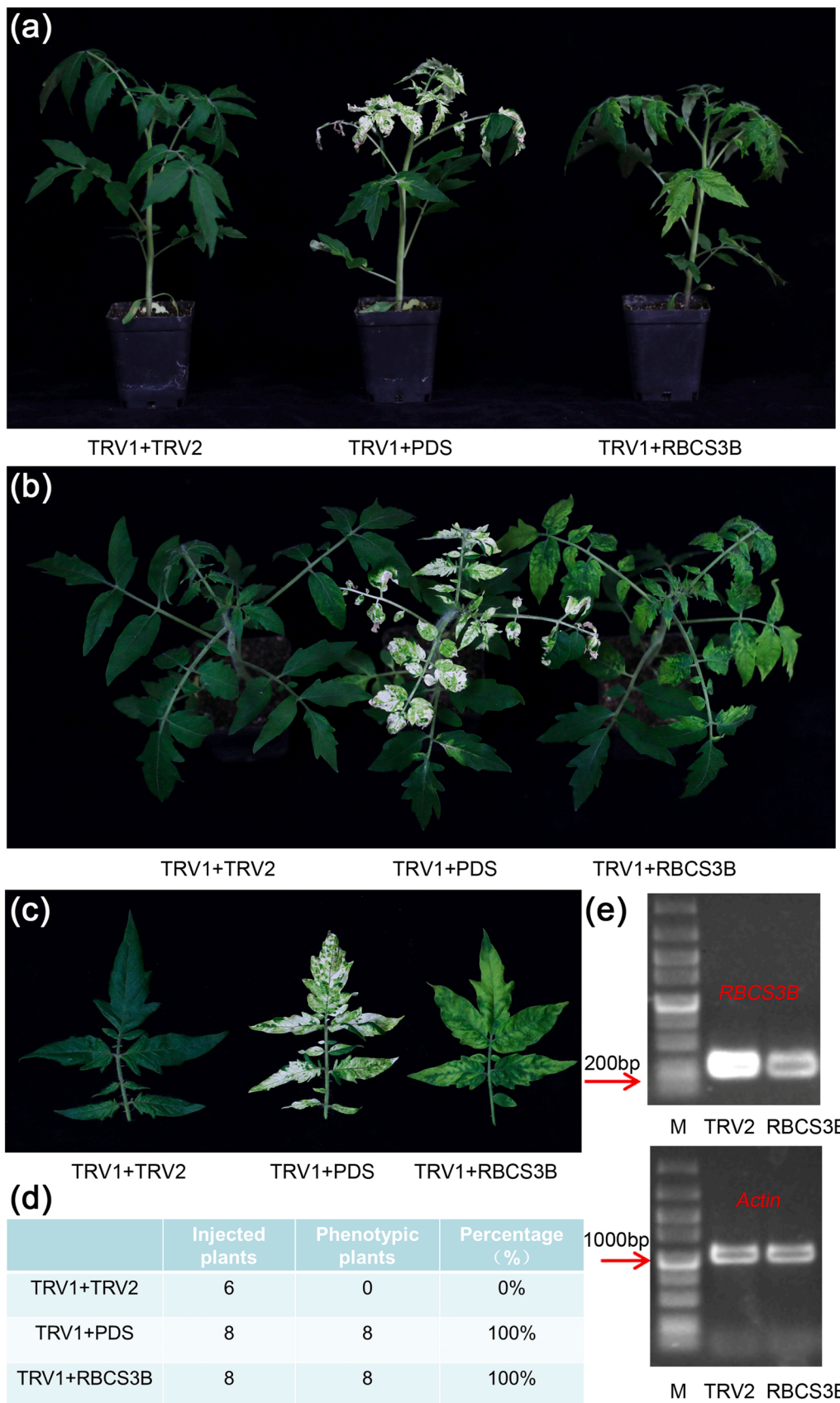


Fig. 6. Phenotypes of tomato plants with the *RBCS3B* gene silenced by VIGS. (a-c) Phenotypes of tomato plants inoculated with *Agrobacterium* strains containing TRV1 + TRV2 (negative control), TRV1 + TRV2-PDS (positive control) and TRV1 + TRV2-RBCS3B. (d) Percentages of visible pale or pale green phenotypes in tomato plants inoculated with *Agrobacterium* strains containing the silencing plasmids. (e) Confirmation of down-regulated *RBCS3B* gene expression by VIGS. The transcript levels of *RBCS3B* was amplified by RT-PCR using RNA extracted from tomato plants inoculated with *Agrobacterium* strains containing TRV1 + TRV2 (negative control) and TRV1 + TRV2-RBCS3B (upper panel). Note that the *RBCS3B* band of about 200 bp is weaker in the VIGS-silenced plant (RBCS3B) than in the control (TRV2). The actin transcript was used as an internal control (lower panel).

Gene expression analysis indicates that the expression of *RBCS3B* was significantly suppressed in the *RBCS3B*-TRV2 plants (Fig. 6d-e). The *RBCS3B*-TRV2 plants became pale green as compared with the TRV2 control plants (Fig. 6a-c). Taken together, our results demonstrate that *SICAT2* mainly functions in ROS scavenging and *RBCS3B* plays an important role in chlorophyll accumulation. We also observed that the expression levels of *CAT2* and *RBCS3B* were significantly decreased in the *MsrB2*-RNAi transgenic lines as compared with those in the WT control, but only *RBCS3B* was significantly increased in *MsrB2*-OE transgenic lines as compared with WT (Fig. S4). Combined with the *SlMsrB2*'s role in ROS scavenging and chlorophyll accumulation (Fig. 3), and its interactions with *SICAT2* or *RBCS3B* (Fig. 4), our results clearly indicate that *SlMsrB2* directly interacts with *SICAT2* and *SlRBCS3B* and participates in ROS scavenging and chlorophyll maintenance during stress in plants.

4. Discussion

Abiotic stresses induce the production of ROS in chloroplasts, mitochondria, and peroxisomes, as well as at the plasma membrane [21, 37–39]. ROS accumulation can not only accelerate photodamage, but also inhibits the repair of photosystem II (PSII) *in vivo* [29]. Accumulation of ROS in cellular compartments results in oxidative stress and affects organelle integrity. Antioxidants, antioxidative enzymes, and scavenging enzymes like catalase (CAT), ascorbate peroxidase (APX), and superoxide dismutase (SOD) can effectively eliminate ROS, leading to the regulation of ROS homeostasis [16,40]. Catalase plays important roles in plant antioxidative and detoxification processes that are closely correlated with ROS generation during photosynthesis and photorespiration [41]. Chloroplast and mitochondria are the main sites for production of endogenous H_2O_2 in plant cells [17,18]. Catalase genes play an essential role during plant growth, development, and response to stress [41]. In *Arabidopsis*, loss of *CAT2* results in an 80% loss of catalase activity and its mutant plants are hypersensitive to high-intensity of light, H_2O_2 , salinity, and cold [20,21,42].

In this study, we found that leaves of *SICAT2* RNAi transgenic lines became pale green with a much lower level of chlorophyll content and a higher level of ROS (Fig. 5, S2). Consistently, the green shoulders of tomato fruits became unevenly pale green and yellow spots appeared on ripen fruits in *SICAT2* RNAi transgenic lines, which are probably caused by ROS accumulation (Fig. S3). These results indicate that *CAT2* plays an important role in the process of growth and development. Possibly due to the constitutively high expression of *SICAT2* in WT plants, we did not find any visible phenotypic changes in the *SICAT2*-OE lines, which is consistent with previous reports on other plant species [20,21,43].

Rubisco has been one of the focuses of biological studies for many decades. As the rate-limiting enzyme of photosynthesis in C3 and C4 crops, it is a potential target for genetic manipulation to increase chlorophyll contents and photosynthetic capacity [27,28]. In this study, we found that suppressing the expression of *RBCS3B* by VIGS method could generate pale green leaves in tomato (Fig. 6). Similar phenotype was also observed in tobacco *RBCS3B* VIGS plants (Fig. S5). In *Arabidopsis*, co-suppression of *RBCS3B* gene results in decrease in the number of chloroplasts per mesophyll cell and the chlorophyll contents [29]. These results illustrate that *RBCS3B* plays conserved roles in photodamage protection among different plant species.

SlMsrB2 is localized to the chloroplast (Fig. 2b-c) and can directly interact with *RBCS3B* *in vitro* and *in planta* (Fig. 4). In chloroplasts, the reaction centers of PSI and PSII in thylakoids are the major sites of ROS generation. Under normal growth conditions, ROS do not accumulate to a high level to avoid causing damages to the cell. However, under biotic or abiotic stresses, ROS could be overproduced to give rise to cellular damages (oxidative stress), even leading to the cell death in severe cases [44]. Our observations have led us to speculate that the *RBCS3B* protein may have its known activity as a small subunit of Rubisco and functions in CO_2 fixation under normal growth conditions. During drought stress,

RBCS3B protein might be gradually damaged by ROS accumulation. At this time, *SlMsrB2* may interact with *RBCS3B* and partially restores its activity, allowing the photosynthesis to proceed smoothly. Under normal conditions, *SlMsrB2* RNAi transgenic lines showed no significant phenotypic difference from WT, but under drought conditions, the chlorophyll content was significantly reduced (Fig. 3b). The expression of *RBCS3B* was significantly down-regulated in the *MsrB2*-RNAi lines and significantly increased in *MsrB2*-OE lines as compared with its expression level in the WT control (Fig. S4). Therefore, the *SlMsrB2* gene seems to affect the chlorophyll content by regulating both the protein activity and gene expression of *RBCS3B*. It is not known how *MsrB2* exerts its role to regulate the expression of the *RBCS3B* gene.

Like its counterpart from *Arabidopsis* (*AtCAT2*), tomato *CAT2* protein was localized in the peroxisome (Fig. S1b), where it interacted with *SlMsrB2*. Because *SlMsrB2* was also localized in the chloroplast (Fig. 2c), it means that *SlMsrB2* is a dual subcellular localization protein, present in both the peroxisome and chloroplast. Dual subcellular localizations of proteins in plant cells are not uncommon. In Fig. 2c, the yellow fluorescence of *MsrB2*-YFP was detected in the chloroplasts, but not in the peroxisome. This could likely be due to the very strong yellow fluorescence signals in the chloroplast that could over-shadow the relatively weak signal from the tiny peroxisomes, which would make it difficult to record the presence of *MsrB2*-YFP in the peroxisomes. This interpretation is consistent with the previous studies by Oikawa [45]. The leaves of *CAT2* RNAi transgenic lines also became pale green along with significantly decreased chlorophyll content, and this was likely due to oxidative stress caused by ROS accumulation (Fig. 5, S2). Therefore, we hypothesize that *CAT2* protein may have its normal enzyme activity and scavenges the ROS in the chloroplasts, mitochondria and other organelles under normal growth conditions. However, during drought stress, *CAT2* could be damaged due to the large amount of ROS, which in turn leads to the stagnation of photosynthesis and stunted growth and development of plants. Our observations show that *MsrB2* can interact with *CAT2* and partially restore the activity of *CAT2*, especially under drought conditions. Our hypothesis is supported by the observation that the *MsrB2* RNAi transgenic lines showed no significant phenotypic changes under normal conditions, while the ROS level was significantly increased in the RNAi lines but reduced in the OE lines under drought conditions (Fig. 3a, d, f). During the course of this research, we also generated F1 hybrid plants and an F2 population (obtained from self-fertilization of F1) from the cross between *MsrB2*-OE and *CAT2*-RNAi. Analysis of the phenotypes of these plants revealed that the pale green leaf phenotype of *CAT2*-RNAi plants could not be restored by overexpression of *MsrB2* (Fig. S6). This result further demonstrates that *MsrB2* plays important roles in maintenance of the chlorophyll content, ROS scavenging and drought tolerance by protecting and maintaining the activity of *CAT2* enzyme.

5. Conclusion

Based on the results of this report, we propose here a model to explain the roles of *MsrB2* in drought tolerance in plants. In this model, there are two patterns of *MsrB2* in regulating ROS scavenging and chlorophyll accumulation (Fig. 7). Under normal growth conditions, *CAT2* and *RBCS3B* display their corresponding enzyme activities (Fig. 7) and the interaction between *MsrB2* and *RBCS3B* or *CAT2* does not affect the growth and development of tomato plants. However, under drought conditions, rapid ROS accumulation may trigger damages to *CAT2* and *RBCS3B* proteins, which further leads to stagnation of photosynthesis and ultimate stunted growth and development of plants (Fig. 7). Under this situation, *MsrB2* begins to recruit and interact with its target proteins *RBCS3B* and *CAT2* to restore their enzyme activities, leading to improved drought tolerance.

In response to oxidative stress, plant cells employ enzymes such as catalase (CAT), ascorbate peroxidase (APX), peroxidase (POD), and superoxide dismutase (SOD) to eliminate ROS and prevent oxidative

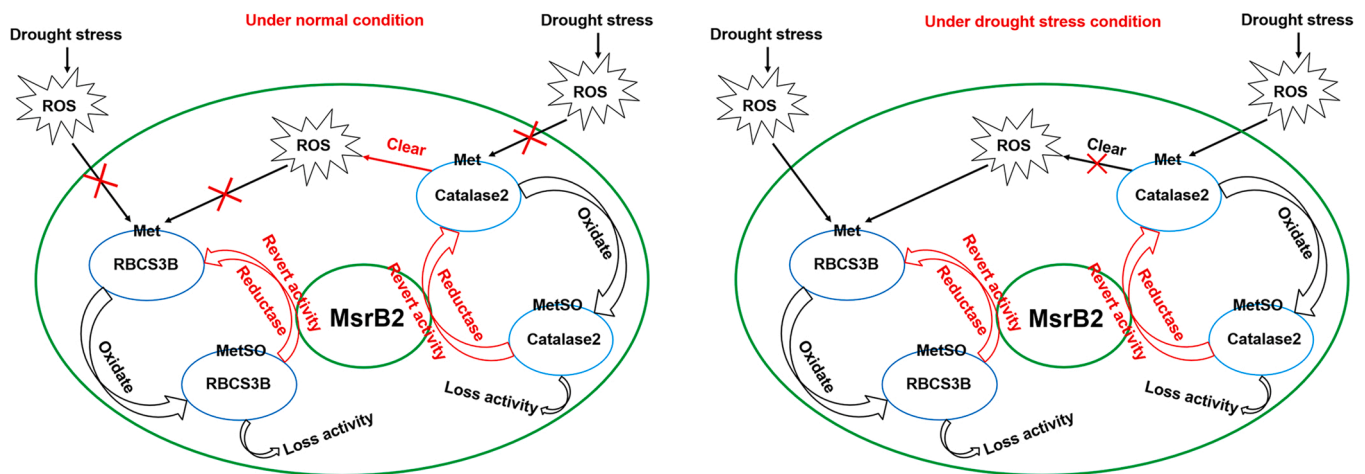


Fig. 7. Proposed model on the role of MsrB2 in drought tolerance in plants. See text for detailed description and discussion.

damages to the cells in the first place. When oxidative stress already causes damages such as the oxidation of Met to MetSO, plants can activate the repair processes such as using the Msr enzyme that can revert the oxidized MetSO back to Met, allowing a damaged protein to recover its activity. Our findings provide new insights into the mechanisms of MsrB2 in improving drought tolerance of tomato plants. This mechanism would have implication in genetic improvement of plant drought tolerance.

CRedit authorship contribution statement

Junhong Zhang, Long Cui and Fangyan Zheng planned and designed the research. Long Cui, Fangyan Zheng, Dedi Zhang, Changxing Li, Miao Li, Jie Ye, Yuyang Zhang and Taotao Wang performed the experiments, conducted fieldwork, analyzed the data and made conclusions based on the results. Long Cui, Bo Ouyang, Zonglie Hong and Junhong Zhang wrote the manuscript.

One-sentence summary

MsrB2 regulates ROS scavenging and chlorophyll accumulation by direct interaction with Catalase 2 and RBCS3B.

Declaration of Competing Interest

The authors declare no competing financial interests.

Acknowledgments

We thank Professor Jihong Liu and Professor Zhengming Wang for critically revising our manuscript and for suggestions. This work was supported by grants from the China Agriculture Research System (CARS-23-A13), the National Natural Science Foundation of China (31772317 and 32072595), the Fundamental Research Funds for the Central Universities (2662020YLPY002) and the China Postdoctoral Science Foundation (2021M691173).

Appendix A. Supporting information

Supplementary data associated with this article can be found in the online version at [doi:10.1016/j.plantsci.2022.111206](https://doi.org/10.1016/j.plantsci.2022.111206).

References

- [1] L.S. Monk, K.V. Fagerstedt, R.M.M. Crawford, Oxygen toxicity and superoxide dismutase as an anti-oxidant in physiological stress, *Physiol. Plant.* 76 (1989) 456–459.
- [2] B. Li, C. Sun, X. Lin, W. Busch, The emerging role of GSNOR in oxidative stress regulation, *Trends Plant Sci.* 26 (2021) 156–168.
- [3] J. Gao, D.H. Yin, Y.H. Yao, H.Y. Sun, Z.H. Qin, C. Schoneich, T.D. Williams, T. C. Squier, Loss of conformational stability in calmodulin upon methionine oxidation, *Biophys. J.* 74 (1998) 1115–1134.
- [4] B. Ezraty, L. Aussel, F. Barras, Methionine sulfoxide reductases in prokaryotes, *Bba-Proteins Prote* 1703 (2005) 221–229.
- [5] E.R. Stadtman, J. Moskovitz, R.L. Levine, Oxidation of methionine residues of proteins: Biological consequences, *Antioxid. Redox, Sign* 5 (2003) 577–582.
- [6] L. Tarrago, E. Laugier, P. Rey, Protein-repairing methionine sulfoxide reductases in photosynthetic organisms: gene organization, reduction mechanisms, and physiological roles, *Mol. Plant.* 2 (2009) 202–217.
- [7] E.R. Stadtman, H. Van Remmen, A. Richardson, N.B. Wehr, R.L. Levine, Methionine oxidation and aging, *Bba-Proteins Prote* 1703 (2005) 135–140.
- [8] R.L. Levine, B.S. Berlett, J. Moskovitz, L. Mosoni, E.R. Stadtman, Methionine residues may protect proteins from critical oxidative damage, *Mech. Ageing Dev.* 107 (1999) 323–332.
- [9] N. Gustavsson, B.P. Kokke, U. Harndahl, M. Silow, U. Bechtold, Z. Poghosyan, D. Murphy, W.C. Boelens, C. Sundby, A peptide methionine sulfoxide reductase highly expressed in photosynthetic tissue in *Arabidopsis thaliana* can protect the chaperone-like activity of a chloroplast-localized small heat shock protein, *Plant J.* 29 (2002) 545–553.
- [10] U. Bechtold, D.J. Murphy, P.M. Mullineaux, Arabidopsis peptide methionine sulfoxide reductase2 prevents cellular oxidative damage in long nights, *Plant Cell* 16 (2004) 908–919.
- [11] H.Y. Ruan, X.D. Tang, M.L. Chen, M.A. Joiner, G.R. Sun, N. Brot, H. Weissbach, S. H. Heinemann, L. Iverson, C.F. Wu, T. Hoshi, High-quality life extension by the enzyme peptide methionine sulfoxide reductase, *P. Natl. Acad. Sci. Usa.* 99 (2002), 7184–7184.
- [12] C.V. Dos Santos, S. Cuine, N. Rouhier, P. Rey, The Arabidopsis plastidic methionine sulfoxide reductase B proteins. Sequence and activity characteristics, comparison of the expression with plastidic methionine sulfoxide reductase A, and induction by photooxidative stress, *Plant Physiol.* 138 (2005) 909–922.
- [13] S.K. Oh, K.H. Baek, E.S. Seong, Y.H. Joung, G.J. Choi, J.M. Park, H.S. Cho, E. A. Kim, S. Lee, D. Choi, CaMsrB2, pepper methionine sulfoxide reductase B2, is a novel defense regulator against oxidative stress and pathogen attack, *Plant Physiol.* 154 (2010) 245–261.
- [14] S.J. Kwon, S.I. Kwon, M.S. Bae, E.J. Cho, O.K. Park, Role of the methionine sulfoxide reductase MsrB3 in cold acclimation in *Arabidopsis*, *Plant Cell Physiol.* 48 (2007) 1713–1723.
- [15] M.J. Rodrigo, J. Moskovitz, F. Salamini, D. Bartels, Reverse genetic approaches in plants and yeast suggest a role for novel, evolutionarily conserved, selenoprotein-related genes in oxidative stress defense, *Mol. Genet. Genom.* 267 (2002) 613–621.
- [16] A. Mhamdi, G. Queval, S. Chaouch, S. Vanderauwera, F. Van Breusegem, G. Noctor, Catalase function in plants: a focus on *Arabidopsis* mutants as stress-mimic models, *J. Exp. Bot.* 61 (2010) 4197–4220.
- [17] J. Dat, S. Vandenabeele, E. Vranova, M. Van Montagu, D. Inze, F. Van, Breusegem, Dual action of the active oxygen species during plant stress responses, *Cell. Mol. life Sci.: CMLS* 57 (2000) 779–795.
- [18] A.P. Moller, T.A. Mousseau, F. de Lope, N. Saino, Elevated frequency of abnormalities in barn swallows from Chernobyl, *Biol. Lett.* 3 (2007) 414–417.
- [19] M. Zamocky, P.G. Furtmuller, C. Obinger, Evolution of catalases from bacteria to humans, *Antioxid. Redox Sign.* 10 (2008) 1527–1548.
- [20] E. Bueso, S. Alejandro, P. Carbonell, M.A. Perez-Amador, J. Fayos, J.M. Belles, P. L. Rodriguez, R. Serrano, The lithium tolerance of the *Arabidopsis cat2* mutant reveals a cross-talk between oxidative stress and ethylene, *Plant J.* 52 (2007) 1052–1065.
- [21] J. Li, J. Liu, G. Wang, J.Y. Cha, G. Li, S. Chen, Z. Li, J. Guo, C. Zhang, Y. Yang, W. Y. Kim, D.J. Yun, K.S. Schumaker, Z. Chen, Y. Guo, A chaperone function of NO

- CATALASE ACTIVITY1 is required to maintain catalase activity and for multiple stress responses in *Arabidopsis*, *Plant Cell* 27 (2015) 908–925.
- [22] Y. Fukamatsu, N. Yabe, K. Hasunuma, *Arabidopsis* NDK1 is a component of ROS signaling by interacting with three catalases, *Plant Cell Physiol.* 44 (2003) 982–989.
- [23] T. Hackenberg, T. Juul, A. Auzina, S. Gwizdz, A. Malolepszy, K. Van Der Kelen, S. Dam, S. Bressendorff, A. Lorentzen, P. Roepstorff, K.L. Nielsen, J.E. Jorgensen, D. Hofius, F. Van Breusegem, M. Petersen, S.U. Andersen, Catalase and *NO CATALASE ACTIVITY1* promote autophagy-dependent cell death in *Arabidopsis*, *Plant Cell* 25 (2013) 4616–4626.
- [24] Y.S. Li, L.C. Chen, J.Y. Mu, J.R. Zuo, LESION SIMULATING DISEASE1 interacts with Catalases to regulate hypersensitive cell death in *Arabidopsis*, *Plant Physiol.* 163 (2013) 1059–1070.
- [25] M.M. Mathioudakis, R.S.L. Veiga, T. Canto, V. Medina, D. Mossialos, A.M. Makris, I. Livieratos, *Pepino mosaic virus* triple gene block protein 1 (TGBp1) interacts with and increases tomato catalase 1 activity to enhance virus accumulation, *Mol. Plant Pathol.* 14 (2013) 589–601.
- [26] T. Yang, B.W. Poovaiah, Hydrogen peroxide homeostasis: activation of plant catalase by calcium/calmodulin, *P. Natl. Acad. Sci. USA* 99 (2002) 4097–4102.
- [27] C.C. Mann, Future food - Bioengineering - Genetic engineers aim to soup up crop photosynthesis, *Science* 283 (1999) 314–316.
- [28] R.J. Spreitzer, M.E. Salvucci, Rubisco: Structure, regulatory interactions, and possibilities for a better enzyme, *Annu. Rev. Plant Biol.* 53 (2002) 449–475.
- [29] G.M. Zhan, R.J. Li, Z.Y. Hu, J. Liu, L.B. Deng, S.Y. Lu, W. Hua, Cosuppression of *RBCS3B* in *Arabidopsis* leads to severe photoinhibition caused by ROS accumulation, *Plant Cell Rep.* 33 (2014) 1091–1108.
- [30] M. Izumi, H. Tsunoda, Y. Suzuki, A. Makino, H. Ishida, *RBCS1A* and *RBCS3B*, two major members within the *Arabidopsis* *RBCS* multigene family, function to yield sufficient Rubisco content for leaf photosynthetic capacity, *J. Exp. Bot.* 63 (2012) 2159–2170.
- [31] B. Jones, P. Frasse, E. Olmos, H. Zegzouti, Z.G. Li, A. Latche, J.C. Pech, Down-regulation of DR12, an auxin-response-factor homolog, in the tomato results in a pleiotropic phenotype including dark green and blotchy ripening fruit, *Plant J.* 32 (2002) 603–613.
- [32] H.K. Lichtenthaler, A.R. Wellburn, Determination of total carotenoids and chlorophylls a and b of leaf in different solvents, *Biochem. Soc. Trans.* 11 (1985) 591–592.
- [33] Q. Zhang, M. Wang, J. Hu, W. Wang, X. Fu, J.H. Liu, PtrABF of *Poncirus trifoliata* functions in dehydration tolerance by reducing stomatal density and maintaining reactive oxygen species homeostasis, *J. Exp. Bot.* 66 (2015) 5911–5927.
- [34] U.K. Shekhawat, L. Srinivas, T.R. Ganapathi, *MusaDHN-1*, a novel multiple stress-inducible SK (3)-type dehydrin gene, contributes affirmatively to drought- and salt-stress tolerance in banana, *Planta* 234 (2011) 915–932.
- [35] P.S. Campos, V. Quartin, J.C. Ramalho, M.A. Nunes, Electrolyte leakage and lipid degradation account for cold sensitivity in leaves of *Coffea* sp. plants, *J. Plant Physiol.* 160 (2003) 283–292.
- [36] J.S. Kim, H.M. Park, S. Chae, T.H. Lee, D.J. Hwang, S.D. Oh, J.S. Park, D.G. Song, C.H. Pan, D. Choi, Y.H. Kim, B.H. Nahm, Y.K. Kim, A pepper *MSRB2* gene confers drought tolerance in rice through the protection of chloroplast-targeted genes, *PLoS One* 9 (2014), e90588.
- [37] J. Foreman, V. Demidchik, J.H.F. Bothwell, P. Mylona, H. Miedema, M.A. Torres, P. Linstead, S. Costa, C. Brownlee, J.D.G. Jones, J.M. Davies, L. Dolan, Reactive oxygen species produced by NADPH oxidase regulate plant cell growth, *Nature* 422 (2003) 442–446.
- [38] R. Mittler, S. Vanderauwera, M. Gollery, F. Van Breusegem, Reactive oxygen gene network of plants, *Trends Plant Sci.* 9 (2004) 490–498.
- [39] S. Munne-Bosch, G. Queval, C.H. Foyer, The impact of global change factors on redox signaling underpinning stress tolerance, *Plant Physiol.* 161 (2013) 5–19.
- [40] R.G. Alscher, J.L. Donahue, C.L. Cramer, Reactive oxygen species and antioxidants: Relationships in green cells, *Physiol. Plant.* 100 (1997) 224–233.
- [41] A. Mhamdi, G. Noctor, A. Baker, Plant catalases: Peroxisomal redox guardians, *Arch. Biochem. Biophys.* 525 (2012) 181–194.
- [42] T. Juul, A. Malolepszy, K. Dybkaer, R. Kidmose, J.T. Rasmussen, G.R. Andersen, H. E. Johnsen, J.E. Jorgensen, S.U. Andersen, The in vivo toxicity of hydroxyurea depends on its direct target catalase, *J. Biol. Chem.* 285 (2010) 21411–21415.
- [43] C.R. McClung, Regulation of catalases in *Arabidopsis*, *Free Radic. Biol. Med.* 23 (1997) 489–496.
- [44] K. Apel, H. Hirt, Reactive oxygen species: metabolism, oxidative stress, and signal transduction, *Annu. Rev. Plant Biol.* 55 (2004) 373–399.
- [45] K. Oikawa, M. Hayashi, Y. Hayashi, M. Nishimura, Re-evaluation of physical interaction between plant peroxisomes and other organelles using live-cell imaging techniques, *J. Integr. Plant Biol.* 61 (2019) 836–852.